

Optimization of Design for Air Gap Sensor Using the Response Surface Methodology

Kitisak Chimklin* and Chatchapol Chungchoo

Department of Mechanical Engineering, Faculty of Engineering, Kasetsart University, Bangkok, Thailand

* Corresponding author. E-mail: kitisak.ch@ku.th DOI: 10.14416/j.asep.2022.01.003

Received: 19 June 2021; Revised: 21 August 2021; Accepted: 21 September 2021; Published online: 12 January 2022

© 2022 King Mongkut's University of Technology North Bangkok. All Rights Reserved.

Abstract

In Hard Disk Drive (HDD) manufacturing, there is always a concern about the cutting defects that are caused by residual cutting chips. Only a small amount of $10\ \mu\text{m}$ chips (act as the air gap) can cause the workpiece to tilt and shift from the correct position, and thus affect the dimension of the workpiece (mainly the Base HDD). For this reason, researchers adapted the adjustable micrometer as a simulation device that resembles the air gap for the design of the Air Gap Sensor Module. The design of experiments using response surface methodology will be studied to confirm the appropriate factors of the prototype. This study reports the optimization of the main factors that affect Air Gap Sensor Module condition: Air Nozzle Diameter $2.303\ \text{mm}$, Air Pressure $0.1\ \text{MPa}$, and Sampling Time $645\ \text{ms}$, which has a high square of the coefficient correlation (R-squared = 99.0%) with a close relationship between gap distance and air pressure. The relationship between these variables is mostly linear. The R-squared error percentage of actual value is less than 0.93% compared to predicted value. The mathematical model results and experimental values were consistent and able to predict response variables. The Air Gap Sensor Module can provide the measurement results in micron accuracy and displays light and beep to confirm as acceptable or reject gap conditions with the uncertainty of measurement $\pm 0.001\ \text{mm}$.

Keywords: Air Gap Sensor, Design of experiments, Response surface methodology, R squared, Uncertainty of measurement, Base Hard Disk Drive fixture

1 Introduction

A small amount of cutting chips between the datum surface and workpiece could cause separation (gap). A little gap of $10\ \mu\text{m}$ can majorly affect machining accuracy, as shown in Figure 1. Thus, the ideal gap is $0\ \mu\text{m}$. At present, the tool being used to remove the unwanted chips is air nozzle. Relating air pressure in the cavity to the gap between nozzle face on datums and Surface of workpiece, was suggested by Michel Dechape [1]; when the gap increases, it decreases air pressure. Research on air gap for non-contact length measurement was presented by [2]. The advantages of air gauging are: 1) Affordable price, 2) Can be measured without contacting workpiece, 3) The accuracy is usually higher than that of contacting mechanical gauges, 4) Easy measuring with probes designed for special works, and 5) Easy tune up of measuring range

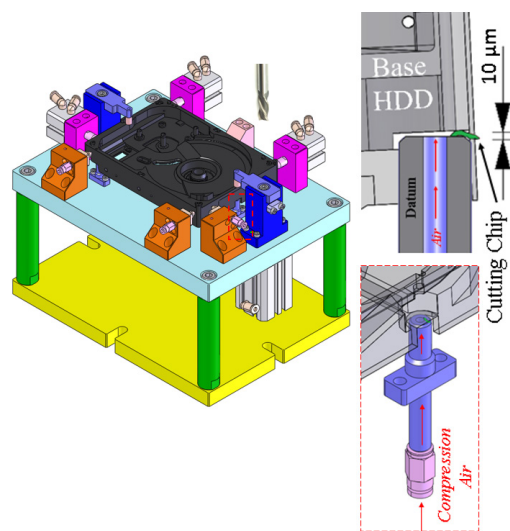


Figure 1: Cutting chips on the datum of fixture.

[3]. In addition, the air from the air gap can blow away the dust if there is dust on the surface of the workpiece. Typically, dimensions of the measuring circular nozzles in air gauge ranges from $\varnothing 1.00$ – $\varnothing 2.00$ mm, using air pressure 0.15 MPa is described in [4]. Therefore, this research study was mainly focused on air nozzle diameter and air pressure. Lastly, the area between the air nozzle and the measurement surface has played a significant role on the measurement result. This result has been examined and are available on the paper [5]. Moreover, the advantage of Response Surface Methodology (RSM) is help minimizing the number of experiment while reducing production cost, time and wastage [6]. Therefore, the RSM that has been proposed in this study, is not only a statistical and mathematical technique for locating optimal conditions, but also analyzing how the appropriate conditions differ in sensitivity between multiple variables. In general, RSM has been used particularly for four-factors, five-levels, central composite rotatable design (CCRD), which are used to optimize the partially epoxidation conditions and study the effect of urea-hydrogen peroxide and methyltrioxorhenium [7]. There were abundant literatures on the use of RSM for optimization and development [8], [9]. Researchers simulated the behavior of the datum point on the fixture, and the factors of the variables are optimized using the Design of Experiments (DOE) by RSM for the design of air gap sensor module, which has a strong correlation. Hence, the results of measurement can be displayed as accurate micron.

2 The Principles and Application

Flow and pressure of controlled compressed air supplied to the system can be interpreted as the relationship between jet nozzle and surface on part. Both simple flow and simple back pressure indicators relationship was discussed in [10].

2.1 Simple flow measuring circuit

In this system, compressed air at a constant, closely controlled pressure is passed through a variable flow meter and then to a suitable nozzle. The air from the nozzle, and if the surface is moved toward or away from the nozzle the flow of air changes and the float in the tube moves accordingly. Calibration can be carried

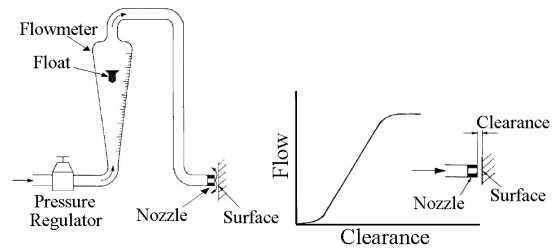


Figure 2: Simple flow system.

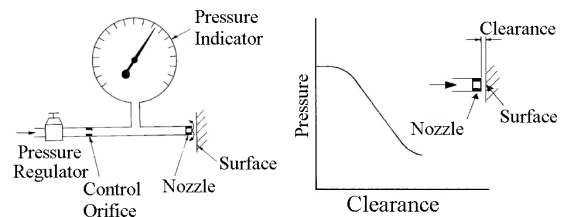


Figure 3: Simple back pressure circuit.

out by applying known displacements to the surface. The graph shown in Figure 2 shows a typical curve shape, relating air flow to the clearance between the nozzle and the surface was discussed in [10].

2.2 Simple back pressure Circuit

In this circuit, compressed air from the pressure regulator passes through the control orifice, before entering the cavity upstream of the escape orifice. Due to the presence of the primary restriction, changes in the restrictive effect of the escape orifice will give rise to changes in pressure in the cavity between the two orifices. Changes in the restrictive effect of the escape orifice are made by moving the surface toward or away from the nozzle face. Changes in pressure inside the cavity can be measured by a pressure indicator such as a Bourdon tube type pressure gauge. Figure 3 shows a typical curve shape relating pressure in the cavity to the clearance between nozzle face and surface. One of the disadvantages of this circuit is that it requires compressed air at a constant, closely controlled pressure; otherwise, the readings will vary proportionately to the variations of the input pressure discussed in [1], [10].

2.3 Response Surface Methodology (RSM)

The RSM is a technique used for simulating and analyzing data to determine the optimal level of factors.

The method works by using mathematical and statistical principles to create a model and analyze problems to find the optimal value of the response which is mostly a problem with the surface responses often unknown the relationship between response and independent variables. Consequently, find suitable approximations to represent the relationship between the response (R^2) and a set of independent variables by using first-degree polynomial that are under certain territories of independent variables. However, curvature in the system requires a higher polynomial usage. The optimum with reasonable precision obtains a general mathematical model was discussed in [11].

3 Materials and Methods

3.1 Materials

The components of the experiment including commercial product and machining part follow designs [12], [13] as shown in Table 1.

Table 1: Material and specification

No.	Material	Model/ Specification	Brand	Country of Manufacturing
1	Digital Micrometer	293-240-30/ 0.001 mm	Mitutoyo	Japan
2	Air Tank	21 litres	Custom	Thailand
3	Regulator	IR1010-01 BG	SMC	Japan
4	Pressure Sensor	ISE40-01 -22-M	SMC	Japan
5	Pressure Sensor	E8EB-01C	OMRON	Japan
6	Air Nozzle Diameter	$\varnothing 1.0, \varnothing 2.0, \varnothing 3.0$ mm	Custom	Thailand
7	Gauge Block	516-903-11	Mitutoyo	Japan
8	Micro Controller	UNO/10-bits	Arduino	USA
9	Analog to Digital Converter (A/D)	16-bits	Custom	Thailand
10	CMM Non-Contact 3D	Hyper Quick Vision	Mitutoyo	Japan
11	Solidworks	Version 2020	Dassault	USA
12	Minitab	Version 2017	Minitab	USA

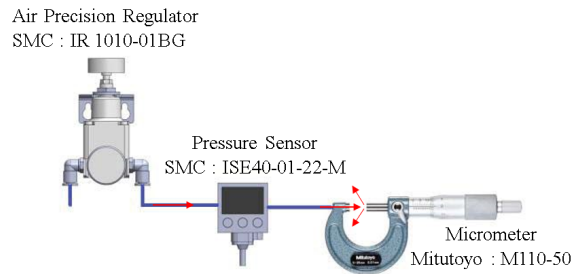


Figure 4: Feasibility of air gauging.

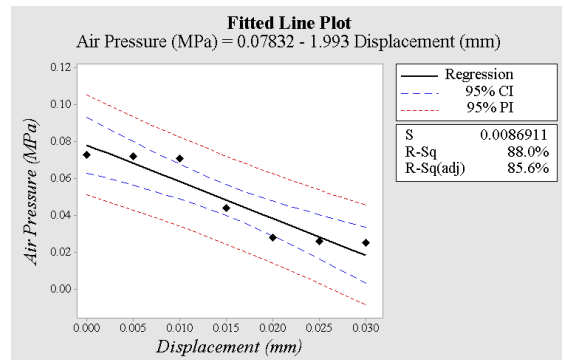


Figure 5: Linear regression using least squares.

3.2 Experimental procedure

3.2.1 Feasibility of theory

In order to prove the reliability of the experiment result. Researcher sets up feasibility of Air gauging an experiment which includes pressure sensor (SMC model ISE40-01-22-M), modify the micrometer at the anvil area by drill to air nozzle id $\varnothing 2.00$ mm and control air pressure at 0.070 MPa by the air precision regulator (SMC model IR 1010-01BG) as shown in Figure 4.

Feasibility of air gauging by the micrometer airhead starts the collection at distance 0 mm and increases 5 μm at a time until 30 μm . Therefore, recording the value to analyze with linear regression analysis as shown in Figure 5. The theoretical truth and show result satisfactory, R square(adj) = 85.6 %, The standard error of the regression (S) = 0.00869, normally S must be less than 2.5 to produce a sufficiently 95% confidence interval confirmed as the model needs to be more precise was provided by Adarsh Menon [14] and Rajesh Gunesh [15].

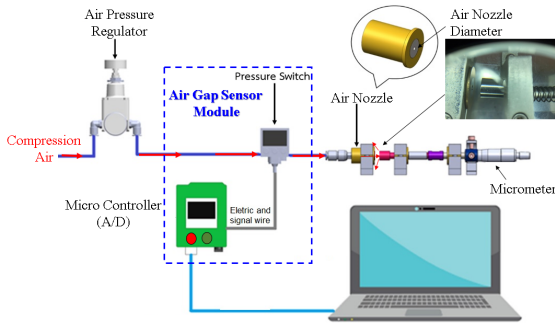


Figure 6: The diagram of prototype.

3.2.2 The prototype substitute the fixture

This research establishes the prototype simulated for the fixture for design of air gap sensor module. The digital micrometer was used in this study represented in the diagram as shown in Figure 6. In addition, the first air nozzle in this study used SKD11 steel, which gave very poor results due to the rust. We changed the material to stainless steel grade SUS304 and controlled the flatness of the surface to ensure the surface between the air nozzle and spindle of micrometer is closed.

3.2.3 Air gap sensor module

Purpose of bringing Microcontroller Arduino Model: UNO due to easy programming and low price. In order to convert signal Analog to Digital (A/D), the experiment to read the pressure values shows that the device is more sensitive to pressure. Due to the pressure sensor sending data into an analog signal that cannot send data directly to the computer. The Microcontroller Arduino has a resolution of 10-bit length and separates the analog voltage (input) by the converter 0–5 V to 2^{10} levels, which are equal to 1,024 levels. That the resolution of this component is very high but not enough for this research. Therefore, A/D converter 16-bit was used to expand the analog voltage (input) between 0 V and 5 V to 2^{16} levels, which are 65,536 levels, were discussed in [16]–[18]. The air gap sensor module displays the results of the measurement as micron with a beep and light decision gap status to Accept show Green color on the other hand Reject show Red color as shown in Figure 7.

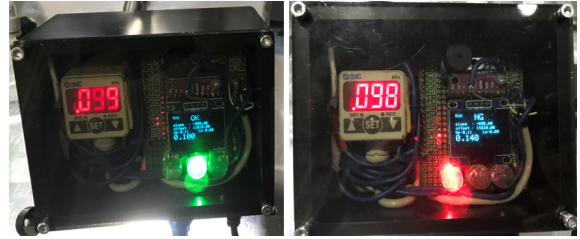


Figure 7: Air gap sensor module with light status.

The main function receives the signal from the Air Pressure Sensor (SMC: ISE40 -01- 22-M), in order to convert A/D signal using Linear regression as indicated in the Equation (1) below,

$$y = mx + c \tag{1}$$

Let y be the A/D value signal (the dependent variable), m be slope, x be the distance value (the independent variable) and c be the y -intercept (offset value) from the equation to show the distance of the signal sent from air gap sensor module as indicated in the Equation (2) below,

$$\text{Distance} = \frac{(\text{Signal A/D}) - (\text{Offset value})}{(\text{Slope})} \tag{2}$$

3.2.4 Determine experimental design type

There are many methodologies available in DOE, i.e. Full factorial design, 2^k factorial method, Taguchi method, and Response surface methodology (RSM). Full factorial design and 2^k factorial method are convenient for a low number of factors if the resources are available. Table 2 shows that the RSM method deploys more experiments than the Taguchi method. The optimization of the RSM result showed that the higher level of factor, the more accurate it is compared to other methods discussed in [19].

Table 2: Number of experiments in each DOE

Factor	Level	Full Factorial (runs)	2^k Factorial (runs)	Taguchi (runs)	RSM (runs)
3	2	8	8	4	20
3	3	27	-	9	20

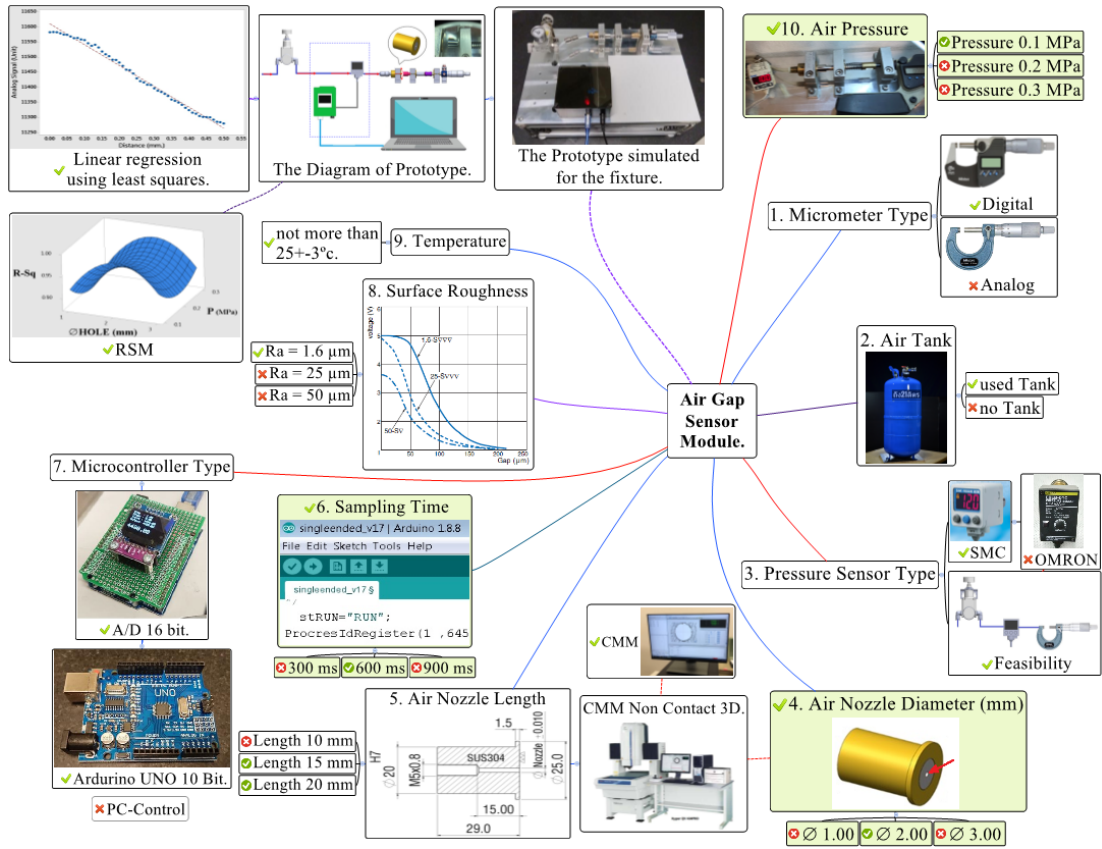


Figure 8: The affect factors for design of the air gap sensor module.

3.2.5 Determine factors and levels

Researchers had re-screened the impact of factors (KPIV) in the Air Gap Sensor Module, benchmarking to analyze the Risk Priority Number (RPN) in Table 4. In order to select the potential factors mentioned shown in Figure 8. Hence, researchers selected 3 important factors to be studied. Also set the level to define parameters in DOE as shown in Table 3.

Table 3: The parameters of the 3 KPIVs in DOE

Factor	Name	Unit	Level of Factor in DOE		
			Low (-1)	Center (0)	High (+1)
A	Air Nozzle Diameter	mm	1.0	2.0	3.0
B	Air Pressure	MPa	0.1	0.2	0.3
C	Sampling Time	ms	300	600	900

Table 4: The RPN affect factors for design

No.	KPIV	Severity (S)	Occurrence (O)	Detection (D)	RPN Score
1	Micrometer Type	8	8	8	512
2	Air Tank	10	9	9	810
3	Pressure Sensor Type	10	9	9	810
4	Air Nozzle Diameter	10	9	9	810
5	Air Nozzle Length	7	7	7	343
6	Sampling Time	10	9	9	810
7	Micro Controller Type	7	7	7	343
8	Surface Roughness	9	6	6	324
9	Temperature	10	7	7	490
10	Air Pressure	10	10	10	1000

4 Experimental and Validation of Results

4.1 Perform experiment using design matrix by RSM

Analysis of Variance (ANOVA) are the conditions using Statistical analysis that create a significant impact on the squared correlation coefficient (R square). Minitab 17 software is capable of performing optimizations on the basis of desired functions. The regression coefficients are performed by testing the significance was discussed in [20]. All factors collected in the corresponding experiment by RSM as listed in the Design matrix shown in Table 5.

ANOVA is used to draw conclusions about the significance of each term in that model. Lack of fit function will remove all non-significant terms. The significant terms reduce the number of models when the mathematical models are defined by the regression coefficients as provided by Ryan [21].

Table 5: Perform experiment using design matrix

Std. Order	Run Order	Pt Type	Air Nozzle Diameter (mm)	Air Pressure (MPa)	Sampling Time (ms)	R Square
1	1	1	1	0.1	300	0.8852
17	2	0	2	0.2	600	0.9814
6	3	1	3	0.1	900	0.9014
15	4	0	2	0.2	600	0.9718
8	5	1	3	0.3	900	0.9059
2	6	1	3	0.1	300	0.9651
3	7	1	1	0.3	300	0.8653
20	8	0	2	0.2	600	0.9806
10	9	-1	3	0.2	600	0.9259
12	10	-1	2	0.3	600	0.9827
14	11	-1	2	0.2	900	0.9297
11	12	-1	2	0.1	600	0.9905
19	13	0	2	0.2	600	0.9484
18	14	0	2	0.2	600	0.9684
16	15	0	2	0.2	600	0.9625
7	16	1	1	0.3	900	0.9038
4	17	1	3	0.3	300	0.9318
13	18	-1	2	0.2	300	0.9366
9	19	-1	1	0.2	600	0.8553
5	20	1	1	0.1	900	0.9169

4.2 Data analysis of R square

From Figure 9, the results of ANOVA for R square showed that the only main factor (Air Nozzle

Response Surface Regression: R2 versus Dia.Hole, Pressure, Time

Backward Elimination of Terms

α to remove = 0.05

Analysis of Variance

Source	DF	Adj SS	Adj MS	F-Value	P-Value
Model	7	0.028679	0.004097	21.31	0.000
Linear	3	0.004699	0.001566	8.15	0.003
Dia.Hole	1	0.004145	0.004145	21.56	0.001
Pressure	1	0.000484	0.000484	2.52	0.138
Time	1	0.000069	0.000069	0.36	0.560
Square	3	0.020788	0.006929	36.04	0.000
Dia.Hole*Dia.Hole	1	0.011575	0.011575	60.20	0.000
Pressure*Pressure	1	0.002664	0.002664	13.85	0.003
Time*Time	1	0.001371	0.001371	7.13	0.020
2-Way Interaction	1	0.003192	0.003192	16.60	0.002
Dia.Hole*Time	1	0.003192	0.003192	16.60	0.002
Error	12	0.002307	0.000192		
Lack-of-Fit	7	0.001544	0.000221	1.45	0.354
Pure Error	5	0.000763	0.000153		
Total	19	0.030986			

Model Summary

S	R-sq	R-sq(adj)	R-sq(pred)
0.0138660	92.55%	88.21%	77.46%

Figure 9: Response surface regression.

Diameter) is statistically significant and also found that the co-factors of Air Nozzle Diameter, Air Pressure and Sampling Time are statistically significant too. It was observed that the p -value was less than 0.05 while R-square(adj) was 88.21%, meaning that the factor selection, factor level and experimental design were well suited [22]

The regression model is developed for the Coefficient of determination shown in the mathematical model, Equation (3). Since the second-order term is significant, it can perform the analysis using an experiment called Response Surface Method in which a variety of experimental designs can be used to analyze quadratic influences or curvature, Central Composite Design (CCD) experimental design is also a popular method, were discussed in [23]. From the analysis of variance all the terms were found to be significant, with the mathematical model in un-coded units below:

$$\text{Coefficient of determination, R square} = 0.6377 + 0.3198 * \text{Air Nozzle Diameter} - 1.315 * \text{Air Pressure} + 0.000422 * \text{Sampling Time} - 0.06488 * \text{Air Nozzle Diameter} * \text{Air Nozzle Diameter} + 3.112 * \text{Air Pressure} * \text{Air Pressure} - 0.000067 * \text{Air Nozzle Diameter} * \text{Sampling Time.} \quad (3)$$

Next, the adequacy of model is investigated by using the residual analysis. The probability plot of residuals indicated that residuals are normally distributed since the p -value of Anderson-Darling

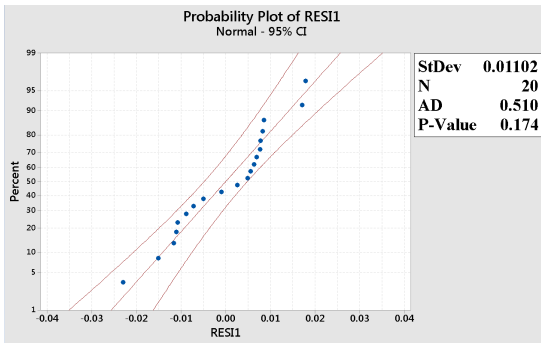


Figure 10: Normality test of residual.

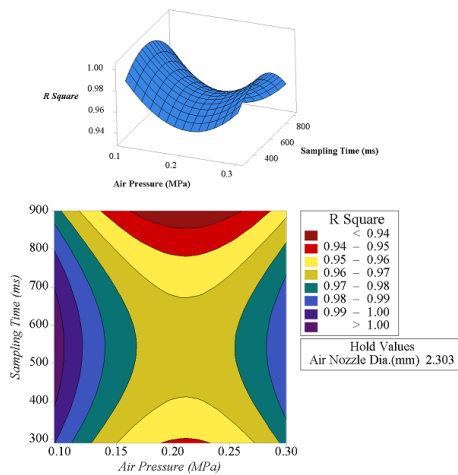


Figure 11: Surface plot relationship of R square, sampling time and air pressure.

(AD) normality test as shown in Figure 10 was greater than the significance level ($\alpha = 0.05$) at confidence level 95% [24].

4.3 Response surface analysis of R square

The mathematical models are power terms of factors making the surface plot curve and when considering the contour plot in Figure 11. The result showed that the curve representing the response variable (y) was an open ellipse curve (dark purple), with the highest response variable. The relationship of interaction between sampling time and air pressure where air nozzle diameter 2.303 mm were considered constant. The result indicated that air pressure of approximately 0.1 MPa and sampling time of approximately 645 ms shows high R square.

The result shown in Figure 12 that curve representing

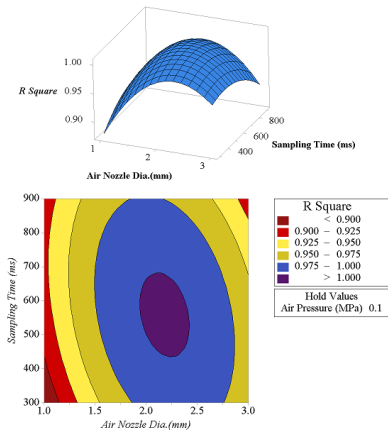


Figure 12: Surface plot relationship of R square, sampling time, air nozzle diameter.

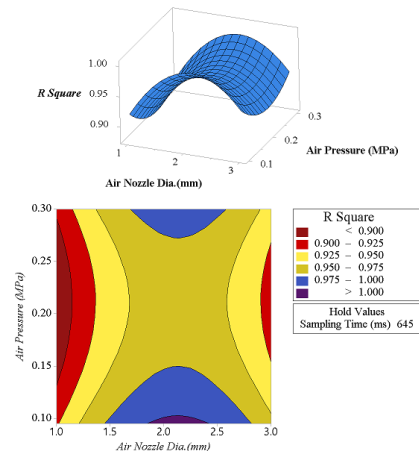


Figure 13: Surface plot relationship of R square, air nozzle diameter, air pressure.

the response variable (y) was closed ellipse curve (dark purple), inside had the highest response variable. The interaction of sampling time and air nozzle diameter. This plot, air pressure 0.1 MPa was considered constant. The result indicated that air nozzle diameter of approximately 2.303 mm and sampling time of approximately 645 ms represent high R square.

The little opened curve (dark purple) and inside had the highest response variable, The interaction of air pressure and air nozzle diameter. This plot, Sampling Time 645 ms were considered constant. The result indicated that air nozzle diameter approximately 2.303 mm and air pressure of approximately 0.1 MPa showed high R square as shown in Figure 13.

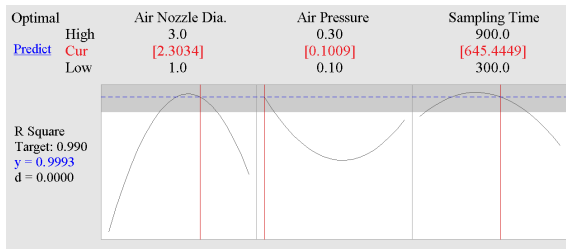


Figure 14: Optimization and predict value.

4.4 Optimization

The response optimizer parameter of factor, recommend the appropriate value for each factor and Predict value with maximum of the R square represent at 0.9993 or 99.93% as shown in Figure 14.

The mathematical model solved by the criteria for optimization which makes the R square highest as shown in Table 6.

Table 6: Criteria for optimization

Factor	Name	Unit	Optimization
A	Air Nozzle Diameter	mm	2.303
B	Air Pressure	MPa	0.1
C	Sampling Time	ms	645

5 Result Validation and Confirmation Data

5.1 Results validation

Take the value obtained from optimization in Table 6 to produce as follows below:

5.1.1 Air nozzle diameter

Researcher produces the air nozzle by controlling the production in making holes diameter 2.303 mm using the wire-cut machine and control length of hole 15 mm with checking all dimensioning by CMM as shown in Figure 15.

5.1.2 Air pressure

Researcher choose to use air pressure 0.1 MPa to setup by rotating the sleeve of micrometer to close completely, then adjust the Air Pressure to the desired pressure at the precision regulator as shown in Figure 16.

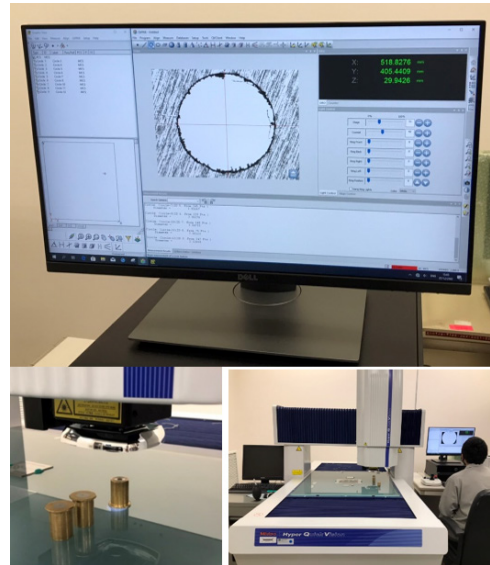


Figure 15: Check dimension of diameter hole.

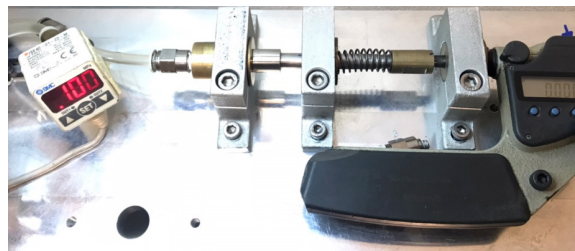


Figure 16: Setup air pressure on 0.1 MPa.

5.1.3 Sampling time

Researcher choose to use sampling time 645 ms to setup by input “645” to Arduino program.

5.2 Confirmation data

Use the optimization of parameters above, obtained from the design of experiments using response surface methodology, setup and finding new linear equations, $y = mx + c$ is analog signal $(y) = 11610 - 690.6$ (Distance) at R-square (adj) 99.00% as shown in Figure 17, input this equation to Arduino program and test runs by using the Gauge block to setup and experiment the next step.

The experimental results from the surface response using Central Composite Design (CCD) method found that factors affecting the coefficient

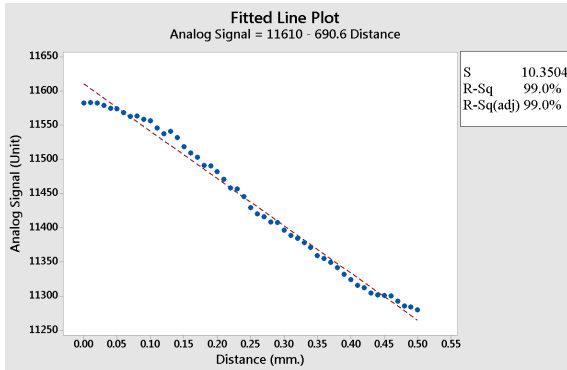


Figure 17: The strength of the relationship.

of determination (R square) this regression equation has suitability for this experiment. A mathematical model performs the Predicted value of the response is obtained, and the best level of the feedback factor is selected by this optimization. Hence, the Percentage error between the Predicted value (shown in Figure 14) and the Actual value (shown in Figure 17) is less than 0.93% which can be acceptable that comparisons are shown in Table 7. The mathematical linear model to predict response variables accurately can be implemented with high confidence.

Table 7: Comparison between Actual value and Predicted value

Responses	Predicted Value	Criteria	Actual Value	Error (%)
R-square (R ²)	0.9993	Maximize	0.9900	0.93

5.3 The calibration of measuring and uncertainty of measurement

Calibration of measuring instruments is to check the measuring instruments that are in the standard of use of that type of measuring instrument or not, in which the calibration is done by referring to the instruments with standard values such as Gauge block, etc. uncertainty of air gap sensor module estimates using statistics usually from repeated readings gap distance = 0.100 mm setting by Gauge block, follow in ISO TAG 4: January 1993. "Guide to the expansion of uncertainty in measurement" were discussed in [25] as shown in Table 8.

Table 8: The calibration and uncertainty of measurement

Times	Gauge Block (mm)	Actual Measured (mm)
1	0.100	0.099
2		0.098
3		0.100
4		0.098
5		0.099
6		0.100
7		0.101
8		0.102
9		0.099
10		0.100
$\bar{x} =$		0.0996
$\sigma =$		0.0013

The uncertainty source, there are 2 types for air gap sensor module: 'Type A' and 'Type B' evaluations. Assessing the uncertainty of both types is necessary.

Type A evaluations: Uncertainty usually from repeated readings by estimates using statistical values as shown in Equation (4).

$$U_A = t \frac{\sigma}{\sqrt{n}} \tag{4}$$

$$U_A = (2.26) \frac{0.0013}{\sqrt{10}} = 0.0009 \text{ mm}$$

σ = Standard deviation = 0.0013 mm
 n = Number of sampling size = 10
 t = 2.26 at Level of confidence 95%

Type B evaluations: Uncertainty base on other data. Data from certificates of calibration, calculations, the old experience of measurement, specifications, published information, and common sense as shown in Equation (5).

$$U_B = \frac{a_w}{2\sqrt{3}} \tag{5}$$

$$U_B = \frac{0.001}{2\sqrt{3}} = 0.00029 \text{ mm}$$

a_w = Resolution Calibration Tester = 0.001 mm

Type A and type B evaluations are calculated by individual standard uncertainty can be combined

using a root sum of the square method. The result is the combined uncertainty of the air gap sensor module there is an error ± 0.001 mm as shown in Equation (6).

$$U_C = \sqrt{U_A^2 + U_B^2} \quad (6)$$

$$U_C = \sqrt{(0.0009)^2 + (0.00029)^2} = \pm 0.001 \text{ mm}$$

6 Conclusions

The optimize the factors affecting the air gap sensor module by using the response surface methodology conditions are: Air nozzle diameter 2.303 mm, air pressure 0.1 MPa, and sampling time 645 ms. The error percentage of R-squared between predicted value and actual value is acceptable at less than 0.93%. Air gap sensor module display light and beep to show accept or reject gap condition with uncertainty of measurement ± 0.001 mm. The result shows 1.0% maximum error on measuring range. Internal diameter measuring head study is recommended for have high accuracy and superior wear resistance.

Acknowledgments

I would like to appreciate the support from Dr. Wiroj Sudatham and Mr. Adithep Jang-on, The National Institute of Metrology (Thailand), and I sincerely thank Dr. Jakawat Deeying and Mr. Torpong Imngern, for supportive suggestions, encouragement, and enthusiasm during study and research work.

References

- [1] M. Dechape, *The Principles and Applications of Pneumatic Gauging*, 2nd ed. Michigan: Society of Manufacturing Engineers, 1983, pp. 88–94.
- [2] S. Laosakulthai, “Design and development of prototype air gauge for non-contacting length measurement optimization,” M.S. thesis, Faculty of Engineering, King Mongkut’s University of Technology North Bangkok, Bangkok, 2015.
- [3] M. Rucki, B. Barisic, and T. Szalay, *Analysis of Air Gage Inaccuracy Causes by Flow Instability*. Amsterdam, Netherlands: Elsevier, 2000, pp. 655–661.
- [4] M. Jukubowicz, “Accuracy of roundness assessment using air gauge with slot-shaped measuring nozzle,” *Measurement*, vol. 155, 2020, Art. no. 107558.
- [5] C. J. Jermak and M. Rucki, “Influence of geometry of the flapper – Nozzle area in the air gauge on its metrological properties,” in *8th International Symposium on Measurement and Quality Control in Production*, 2004, pp. 385–393.
- [6] U. N. Wanasundara and F. Shahidi, “Concentration of omega 3-polyunsaturated fatty acids of seal blubber oil by urea complexation: Optimization of reaction conditions,” *Food Chemistry*, vol. 65, pp. 41–49, 1999.
- [7] Y. N. Lye, N. Salih, and J. Salimon, “Optimization of partial epoxidation on jatropha curcas oil based methyl linoleate using urea-hydrogen peroxide and methyltrioxorhenium catalyst,” *Applied Science and Engineering Progress*, vol. 14, no. 1, pp. 88–99, 2021, doi: 10.14416/j.asep.2020.12.006.
- [8] M. Bahadi, N. Salih, and J. Salimon, “D-optimal design optimization for the separation of oleic acid from malasian high free fatty acid crude plam oil fatty acids mixture using complex fractionation,” *Applied Science and Engineering Progress*, vol. 14, no. 2, pp. 175–186, 2021, doi: 10.14416/j.asep.2021.03.004.
- [9] A. Hamisu and U. I. Gaya, “Bi-template assisted sol-gel synthesis of photocatalytically-active mesoporous anatase TiO₂ nanoparticles,” *Applied Science and Engineering Progress*, vol. 14, no. 3, pp. 313–327, 2021, doi: 10.14416/j.asep.2021.04.003.
- [10] M. Dechape, “Pneumatic gauging system A.K.A. air gauging system A.K.A. air electric converter,” U.S. Patent 7 694 549 B2, 2010.
- [11] P. Pongdang, “Improvement of pivot assembly process using response surface methodology,” M.S. thesis, Faculty of Engineering, Thammasat University, Bangkok, 2018.
- [12] *Slim Pressure Sensor Model*, Omron E8EB-01C, 2021.
- [13] *Digital Pressure Switch Model*, SMC ISE40-01-22-M, 2021.
- [14] A. Menon, “Linear Regression Using Least Squares,” 2018. [Online]. Available: <https://towardsdatascience.com/linear-regression-using-least-squares-a4c3456e8570>.
- [15] R. Gunesh, “Correlation Analysis,” 2020. [Online]. Available: <https://www.rajgunesh.com/resources/>

- downloads/statistics/pearsoncorrel.pdf
- [16] Micro controller Board, “Analog to Digital Converter tutorial,” 2020. [Online]. Available: <http://www.microcontrollerboard.com/analog-to-digital-converter>.
- [17] Custom Control Sensors, “What’s the Difference Between a Pressure Switch and Sensor,” 2014. [Online]. Available: <https://www.ccsdualsnap.com/pressure-switches-vs-pressure-transmitters>.
- [18] RS Components, “Pressure Gauge Type,” 2020. [Online]. Available: <https://th.rs-online.com/web/c/pneumatics-hydraulics/pneumatic-hydraulic-pressure-gauges/pressure-gauges/>.
- [19] D. C. Montgomery, *Design and Analysis of Experiments*, 8th ed. New York: John Wiley & Sons, 2012.
- [20] B. F. Ryan, B. L. Joiner, and J. D. Cryer, *MINITAB Handbook Update for Release 16*, 6th ed. California: Brooks/Cole Publishing Co., 2010.
- [21] J. Deeying, “Optimization of process parameters in lead-free solder jet bonding using laser to increase the shear strength of solder joint in HGA,” Ph.D. dissertation, Faculty of Engineering, King Mongkut’s University of Technology North Bangkok, Bangkok, 2019.
- [22] S. Pumkrachang, “Multi - objective optimization of UV spot curing technique of slider suspension attachment process using response surface methodology,” Ph.D. dissertation, Faculty of Engineering, King Mongkut’s University of Technology North Bangkok, Bangkok, 2021.
- [23] J. Arnthong, “Optimization of glucoamylase production by a thermotolerant *Rhizopus microsporus* TISTR 3518 using response surface methodology,” in *47th Kasetsart University Annual Conference*, 2018, 112–121.
- [24] B. Durakovic, “Design of experiments application, concepts, examples: State of the art,” *Periodicals of Engineering and Natural Sciences*, vol. 5, no. 3, pp. 421–439, 2017.
- [25] S. Bell, *Measurement Good Practice Guide No.11 (Issue 2) A Beginner’s Guide to Uncertainty of Measurement*. London, UK: The National Physical Laboratory, 2001.